Table 1. *Changes in HR and MAP in coronary artery occlusion*

	120 min Coronary Occlusion								
	C	5	15	30	45	60	75	90	105
HR, beats/min	268±7	264±8	242±8*	250±3*	253±4*	252±4*	250±4*	251±3*	248±4*
MAP, mmHg	84±4	74±5*	69±5*	71±5*	68±5*	67±5*	66±4*	65±4*	64±5*
	60 min Occlusion - 60 min Reperfusion								
	C	5	15	30	45	R5	R15	R30	R45
HR, beats/min	274±9	261±6*	255±7*	254±6*	261±7*	256±5*	263±10*	264±12*	263±9*
MAP, mmHg	78±4	67±3*	65±2*	67±2*	65±2*	61±2*	60±3*†	61±2*	58±2*†

Values are mean ± SE. Data were obtained during control (C), after 5, 15, 30, 45, 60, 75, 90, and 105 min of coronary artery occlusion, and after 5, 15, 30, and 45 min of reperfusion (R). *$P < 0.05$ vs. control. †$P < 0.05$ vs. 45 min occlusion.

coronary occlusion was detected as a whole, the Newman-Keuls test was applied to determine which mean values differed significantly from each other (40). Statistical significance was defined as $P < 0.05$. Values are means ± SE.

RESULTS

Time Course of HR and MAP

Table 1 shows the time courses of HR and MAP during coronary occlusion and reperfusion. Coronary occlusion decreased HR and MAP. Reperfusion did not alter HR but temporarily decreased MAP.

Time Course of Dialysate Lactate, Glycerol, and Myoglobin Levels During Myocardial Ischemia

Coronary occlusion significantly altered dialysate myoglobin levels (Fig. 2). Dialysate myoglobin levels increased significantly from 168 ± 32 ng/ml in the control to 570 ± 107 ng/ml at 0–15 min of occlusion. During 60 min of coronary occlusion, dialysate myoglobin levels progressively increased and reached 2,583 ± 208 ng/ml at 45–60 min of occlusion. A significant increase in blood myoglobin occurred at 45–60 min of coronary occlusion. Dialysate lactate levels were 1.00 ± 0.21 mmol/l in the control and increased after coronary occlusion (Fig. 3). During 60 min of coronary occlusion, dialysate lactate levels markedly increased and reached 3.34 ± 0.50 mmol/l at 45–60 min of occlusion. During 60 min of coronary occlusion, dialysate glycerol levels also increased and reached 232 ± 33 μmol/l at 45–60 min of occlusion.

Time Course of Dialysate Myoglobin Levels During 60 min of Reperfusion Following 60 and 120 Minutes of Ischemia

There were no significant differences in the control dialysate myoglobin levels between the two groups (Fig. 4). During ischemia, the dialysate myoglobin levels progressively increased and reached 4,054 ± 659 ng/ml at 105–120 min of coronary occlusion. During 60 min of coronary occlusion, there were no statistically significant differences in the dialysate myoglobin levels between the two groups. After release of the occluder, the dialysate myoglobin levels markedly increased to 12,569 ± 2,347 ng/ml at 0–15 min of reperfusion. The dialysate myoglobin levels at 0–15 min of reperfusion were fivefold higher than those at 60–75 min of 120 min of coronary occlusion. Furthermore, these values were higher than peak levels during 120 min of coronary occlusion. The

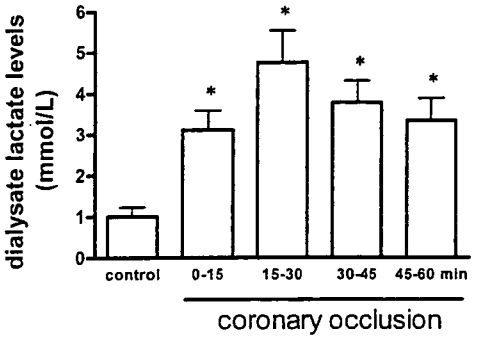

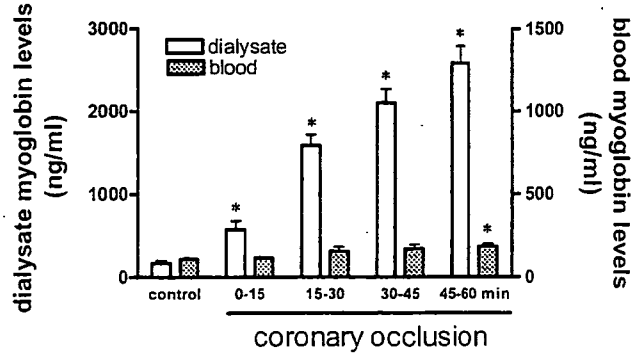

Fig. 2. Time courses of dialysate and blood myoglobin levels during 60 min of ischemia. Values are means ± SE. *$P < 0.05$ vs. control.

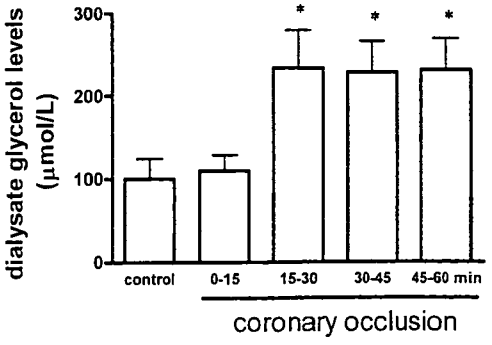

Fig. 3. Time courses of dialysate lactate (*top*) and glycerol (*bottom*) levels during 60 min of ischemia. Values are means ± SE. *$P < 0.05$ vs. control.

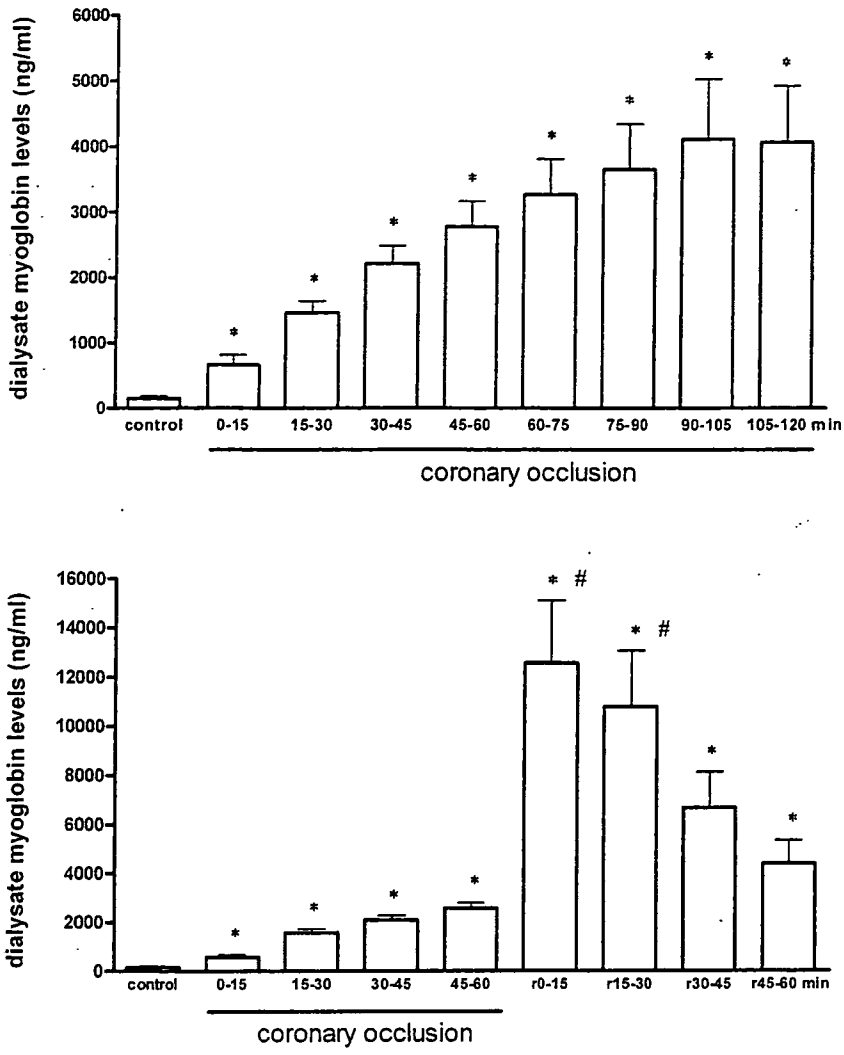

Fig. 4. Time courses of dialysate myoglobin levels during 120 min of ischemia (*top*) and 60 min of ischemia followed by 60 min of reperfusion (r, *bottom*). Values are means ± SE. $^{*}P < 0.05$ vs. control. $^{\#}P < 0.05$ vs. 45–60 min of occlusion.

dialysate myoglobin levels gradually decreased and reached 4,391 ± 879 ng/ml at 45–60 of reperfusion. At 0–15 min of reperfusion, dialysate lactate and glycerol levels were 3.27 ± 0.61 mmol/l and 242 ± 37.7 μmol/l, respectively. Dialysate lactate and glycerol levels remained unchanged at 0–15 min of reperfusion.

Time Course of Dialysate Myoglobin Levels During Local Administration of NaCN

Local administration of NaCN increased the dialysate myoglobin levels (Fig. 5). This increase was statistically significant compared with the control level at all collection periods during NaCN administration, except at 0–15 min. The maximum myoglobin level was comparable to that observed during 60 min of ischemia.

DISCUSSION

Using the dialysis technique in the in vivo rabbit heart, we observed myocardial interstitial myoglobin levels during myocardial ischemia and reperfusion. Our data demonstrated myoglobin release in the early stage of cardiac ischemia and its enhancement by reperfusion. We discuss here the time course of myocardial myoglobin release during coronary occlusion and after reperfusion.

We show for the first time that myoglobin release increases within 15 min of ischemia and continues to increase during 60 min of ischemia. However, significant changes in the blood myoglobin level occurred at 45–60 min of coronary occlusion. Our data suggest a contrast between blood and dialysate

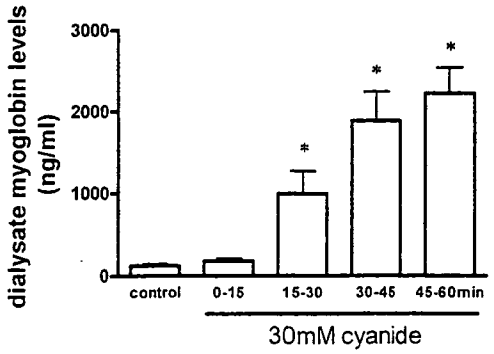

Fig. 5. Time course of dialysate myoglobin levels during local administration of sodium cyanide (30 mM). Values are means ± SE. $^{*}P < 0.05$ vs. control.

myoglobin levels during ischemia. The delay of the first appearance of myoglobin in the bloodstream is mainly due to the slow transport of myoglobin from the interstitial space into the bloodstream (20). Therefore, myoglobin concentration measured by cardiac microdialysis provides information regarding early release of cytosol protein into the interstitial space. Within the 15-min time resolution, this increase in myoglobin release was accompanied by increases in interstitial lactate. Dead space volume between the dialysis fiber and the sample microtube was identical for lactate, glycerol, and myoglobin. The currently accepted concept (20) is that leakage of anaerobic metabolites precedes macromolecular protein release during ischemia. Anaerobic metabolites accumulate and leak from the ischemic region within minutes via diffusion or transport (6, 12, 41). In contrast to low-molecular-weight metabolites, macromolecular proteins could be released into the interstitial space without cytosol accumulation of myoglobin, probably via bleb or altered permeability. Although sampling periods of 15 min are too long to enable us to distinguish the rate of release of lactate vs. myoglobin, our data at least suggest that cellular metabolic derangement is involved in membrane disruption for myoglobin release.

Myocardial injury caused by ischemia-reperfusion is associated with membrane phospholipid degradation, which is thought to underlie disruption of the cell membrane (27). Glycerol is an end product of membrane phospholipid degradation and has been used to study membrane phospholipid degradation after cerebral ischemia and seizures (12). In the present study, dialysate glycerol was examined as a potential marker for membrane phospholipid degradation in myocardial ischemia and reperfusion. We observed increases in dialysate glycerol levels during 15–60 min of ischemia but not during reperfusion. In general, phospholipid degradation is accentuated during reperfusion (27). Therefore, dialysate glycerol is not suitable as an index of membrane phospholipid degradation, and the release of glycerol from membrane phospholipid degradation might be too small to allow detection in blood-perfused heart.

Early change of cytosol myoglobin was detected by immunofluorescence after occlusion of the coronary artery (16, 25). Histochemical studies demonstrated that intracellular diffusion of cytosol myoglobin into the nuclei and mitochondria was evident as early as 0.5 h after coronary artery occlusion (17, 25). Our data demonstrate early loss of cytosol myoglobin into the interstitial space. Release of cytosol protein is caused by membrane damage via alteration of permeability or bleb formation. Blebs appeared on the cell surfaces, and the cell began to swell within 10–20 min of ATP depletion in a glia cell line or hepatocytes (13, 24). Furthermore, NMR spectroscopy suggested that sarcolemmal membranes are gradually permeabilized to large molecules by ischemia (3). These alterations of sarcolemmal membranes might be involved in early release of myoglobin during the myocardial ischemia. Our method offers extremely fast and sensitive analysis of membrane injury in myocardial ischemia that is not evident by histological or blood analysis. Quantitative assessment of interstitial myoglobin levels could be performed independently of reperfusion cell injury and could be helpful in devising various myocardial preservation treatments.

We show that reperfusion markedly accelerates myoglobin release in the ischemic region. The interstitial myoglobin levels at 0–15 min of reperfusion were fivefold higher than those at 60–75 min of 120 min of coronary occlusion. During the reperfusion period, interstitial accumulated myoglobin might be washed out into the bloodstream (37). Therefore, the amount of released myoglobin at reperfusion could be markedly greater than the changes in interstitial myoglobin concentrations at reperfusion. Release of cytosolic protein resulted from a disruption of a sarcolemmal bleb or an enhancement of membrane permeability (5, 29, 35). Either condition may gain relevance during the reperfusion period. Thus the release of myoglobin during the reperfusion seems to serve as an index of disrupted sarcolemmal membrane.

Although the exact mechanisms of accelerated myoglobin release cannot be determined from the present study, our data suggest that substances induced during reperfusion differ from those induced during ischemia. Reperfusion enhanced myoglobin release but did not accelerate lactate or glycerol release in the interstitial space, whereas ischemia accompanied macromolecular myoglobin release as well as anaerobic metabolite release. Furthermore, in the previous studies, neither catecholamine nor acetylcholine release was accelerated by reperfusion in ischemic cardiac sympathetic and parasympathetic nerve endings (2, 14). During reperfusion, surviving myocardial cells and nerve terminals quickly recover aerobic metabolism and take up these accumulated substances, whereas myocardial cells have no capability of myoglobin uptake via the sarcolemmal membrane, leading to continued myoglobin release via the disrupted membrane. Reperfusion may enhance membrane permeability (5). Further disruption of membrane blebs may cause rupture of the membrane (29, 35). Alternatively, in isolated perfused rats, leakage of cytoplasmic enzymes during reoxygenation is accelerated by cardiac revived beating, because the cell membrane becomes fragile during the preceding anoxia (36). In either condition, reperfusion-induced breakdown of membrane phospholipids contributes to an alteration of permeability or bleb formation (27). Disruption of the membrane phospholipid bilayer is likely to play a role in myoglobin release from the cyotosome into the interstitial spaces.

In the present study, we demonstrate that loss of cytosol myoglobin occurs during myocardial ischemia and reperfusion and might be involved in the outcome and pathophysiology of the ischemic heart. Loss of cytosol myoglobin may precede, at least in part, histological evidence of necrosis and occur in the remaining viable myocardium that is not necrotic (11). In vertebrate heart, myoglobin is involved in the transport of oxygen from the sarcolemma to the mitochondria (42). Recent studies from myoglobin knockout mice indicate that myoglobin contributes to the scavenging of bioactive nitric oxide (NO) or oxygen radicals during ischemia-reperfusion (9, 10). NO production and/or oxidant injury occur during the reperfusion period. In hearts lacking myoglobin, changes in NO and oxidative stress have a much larger impact on the maintenance of vascular tone and cardiac function (44). Similarly, in myoglobin knockout mice, loss of cytosol myoglobin may be involved in the delayed restoration of cardiac contractility in the postischemic region.

There are several limitations to the present study. First, with application of the dialysis technique to the heart, we had to perform this experiment as an acute surgical preparation. Probe implantation and/or surgical preparation might affect the con-

centration of myocardial interstitial myoglobin. To examine the effect of probe implantation and/or surgery, we performed the preliminary experiment on brief occlusion (3 min). Three minutes of coronary occlusion did not alter dialysate myoglobin levels. Furthermore, to confirm whether the dialysate myoglobin level reflects myocardial damage evoked by ischemia or hypoxia, we tested the effect of local NaCN administration on dialysate myoglobin levels: with NaCN, we found increases in dialysate myoglobin levels similar to the increase evoked by myocardial ischemia. Therefore, we believe that dialysate myoglobin levels reflect the release of myoglobin evoked by ischemia as well as by chemical hypoxia. The absolute myoglobin level might be affected by implantation and/or surgical preparation. However, it is possible to estimate myoglobin release from relative changes in myoglobin levels.

Second, in the present study, myocardial interstitial myoglobin levels during coronary occlusion and reperfusion were determined regionally. We implanted the dialysis probe in the midwall of the left ventricle. When the dialysis probe was implanted in the subendocardial zone, it is likely that subendocardial ischemia was much more severe than in the midwall, where the sampling was performed. Actually, subendocardial lactate was significantly greater than epicardial lactate during severe ischemia in the anesthetized dogs (6). Further studies are warranted concerning the influence of the ischemic area (subendocardial or marginal zone) on its myocardial interstitial myoglobin levels.

In summary, this microdialysis study in an ischemic animal model shows that coronary occlusion induced myoglobin release in minutes. Micromolecular metabolite (lactate) and macromolecular protein (myoglobin) increased during the first 15 min of ischemia. Reperfusion markedly enhanced myoglobin release without increases in lactate or glycerol levels. Elevation of myoglobin release represents an increase in sarcolemmal permeability or bleb formation during ischemia and reperfusion. Massive disruption of myocardial membrane occurs immediately after ischemia and is markedly accelerated by reperfusion. The dialysis technique permits more concise in vivo monitoring of myocardial membrane disruption during ischemia and reperfusion separately.

GRANTS

This study was supported by the Program for Promotion of Fundamental Studies in Health Science of the Organization for Pharmaceutical Safety and Research by grants-in-aid for scientific research from the Ministry of Education, Science.

REFERENCES

1. **Akiyama T, Yamazaki T, and Ninomiya I.** In vivo monitoring of myocardial interstitial norepinephrine by dialysis technique. *Am J Physiol Heart Circ Physiol* 261: H1643–H1647, 1991.
2. **Akiyama T, Yamazaki T, and Ninomiya I.** Differential regional response of myocardial interstitial noradrenaline levels to coronary occlusion. *Cardiovasc Res* 27: 817–822, 1993.
3. **Askenasy N, Vivi A, Tassini M, Navon G, and Farkas DL.** NMR spectroscopic characterization of sarcolemmal permeability during myocardial ischemia and reperfusion. *J Mol Cell Cardiol* 33: 1421–1433, 2001.
4. **Block MI, Said JW, Siegel RJ, and Fishbein MC.** Myocardial myoglobin following coronary artery occlusion. An immunohistochemical study. *Am J Pathol* 111: 374–379, 1983.
5. **Camilleri JP, Joseph D, Amat D, and Fabiani JN.** Impaired sacrolemmal membrane permeability in reperfused ischemic myocardium. Ultrastructual tracer study. *Virchows Arch* 388: 69–76, 1980.
6. **Delyani JA and Van Wylen GDL.** Endocardial and epicardial interstitial purines and lactate during graded ischemia. *Am J Physiol Heart Circ Physiol* 266: H1019–H1026, 1994.
7. **Dominici R, Infusino I, Valente C, Moraschineli I, and Franzini C.** Plasma or serum samples: measurements of cardiac troponin T and of other analytes compared. *Clin Chem Lab Med* 42: 945–951, 2004.
8. **Farb A, Kolodgie FD, Jones RM, Jenkins M, and Virmani R.** Early detection and measurement of experimental myocardial infarcts with horseradish peroxidase. *J Mol Cell Cardiol* 25: 343–353, 1993.
9. **Flögel U, Gödecke A, Klotz LO, and Schrader J.** Role of myoglobin in the antioxidant defense of the heart. *FASEB J* 18: 1156–1158, 2004.
10. **Flögel U, Merx MW, Gödecke A, Decking UKM, and Schrader J.** Myoglobin: a scavenger of bioactive NO. *Proc Natl Acad Sci USA* 98: 735–740, 2001.
11. **Heyndrickx GR, Amano J, Kenna T, Fallon JT, Patrick TA, Manders WT, Rogers GG, Rosendorff C, and Vatner SF.** Creatine kinase release not associated with myocardial necrosis after short periods of coronary artery occlusion in conscious baboons. *J Am Coll Cardiol* 6: 1299–1303, 1985.
12. **Hillered L, Valtysson J, Enblad P, and Persson L.** Interstitial glycerol as a marker for membrane phospholipid degradation in the acutely injured human brain. *J Neurol Neurosurg Psychiatry* 64: 486–491, 1998.
13. **Jurkowitz-Alexander MS, Altschuld RA, Hohl CM, Johnson JD, McDonald JS, Simmonds TD, and Horrocks LA.** Cell swelling, blebbing, and death are dependent on ATP depletion and independent of calcium during chemical hypoxia in a glial cell line (ROC-1). *J Neuorchem* 59: 344–352, 1992.
14. **Kawada T, Yamazaki T, Akiyama T, Sato T, Shishido T, Inagaki M, Sugimachi M, and Sunagawa K.** Differential acetylcholine release mechanisms in the ischemic and non-ischemic myocardium. *J Mol Cell Cardiol* 32: 405–414, 2000.
15. **Kennergren C, Nyström B, Nyström U, Berglin E, Larsson G, Mantovani V, Lönnroth P, and Hamberger A.** In situ detection of myocardial infarction in pig by measurements of asparate aminotransferase (ASAT) activity in the interstitial fluid. *Scand Cardiovasc J* 31: 343–349, 1997.
16. **Kent SP.** Diffusion of myoglobin in the diagnosis of early myocardial ischemia. *Lab Invest* 46: 265–270, 1982.
17. **Kent SP.** Intracellular diffusion of myoglobin. A manifestation of early cell injury in myocardial ischemia in dogs. *Arch Pathol Lab Med* 108: 827–830, 1984.
18. **Laperche T, Steg PG, Dehoux M, Benessiano J, Grollier G, Aliot E, Mossard JM, Aubry P, Coisne D, Hanssen M, and Iliou MC.** A study of biochemical markers of reperfusion early after thrombolysis for acute myocardial infarction. The PERM Study Group Prospective Evaluation of Reperfusion Markers. *Circulation* 92: 2079–2088, 1995.
19. **Le Quellec A, Dupin S, Genissel P, Savin S, Marchand B, and Houin G.** Microdialysis probes calibration: gradient and tissue dependent changes in no net flux and reverse dialysis methods. *J Pharmacol Toxicol Methods* 33: 11–16, 1995.
20. **Mair J.** Tissue release of cardiac markers: from physiology to clinical applications. *Clin Chem Lab Med* 37: 1077–1084, 1999.
21. **Matsumura K, Jeremy RW, Schaper J, and Becker LC.** Progression of myocardial necrosis during reperfusion of ischemic myocardium. *Circulation* 97: 795–804, 1998.
22. **Miura T.** Does reperfusion induce myocardial necrosis? *Circulation* 82: 1070–1072, 1990.
23. **Nachlas MM and Shnitka TK.** Macroscopic identification of early myocardial infarcts by alterations in dehydrogenase activity. *Am J Pathol* 42: 379–405, 1963.
24. **Nieminen AL, Gores GJ, Wray BE, Tanaka Y, Herman B, and Lemasters JJ.** Calcium dependence of bleb formation and cell death in hepatocytes. *Cell Calcium* 9: 237–246, 1988.
25. **Nomoto K, Mori N, Miyamoto J, Shoji T, and Nakamura K.** Relationship between sarcolemmal damage and appearance of amorphous matrix densities in mitochondria following occlusion of coronary artery in rats. *Exp Mol Pathol* 51: 231–242, 1989.
26. **Ortmann C, Pfeiffer H, and Brinkmann B.** A comparative study on the immunohistochemical detection of early myocardial damage. *Int J Legal Med* 113: 215–220, 2000.
27. **Prasad MR, Popescu LM, Moraru II, Liu X, Maity S, Engelman RM, and Das DK.** Role of phospholipases A_2 and C in myocardial ischemic reperfusion injury. *Am J Physiol Heart Circ Physiol* 260: H877–H883, 1991.

28. **Remppis A, Scheffold T, Greten J, Haass M, Greten T, Kubler W, and Katus HA.** Intracellular compartmentation of troponin T: release kinetics after global ischemia and calcium paradox in the isolated perfused rat heart. *J Mol Cell Cardiol* 27: 793–803, 1995.
29. **Sage MD and Jennings RB.** Cytoskeletal injury and subsarcolemmal bleb formation in dog heart during in vitro total ischemia. *Am J Pathol* 133: 327–337, 1988.
30. **Sarrafzadeh AS, Sakowitz OW, Kiening KL, Benndorf G, Lanksch WR, and Unterberg AW.** Bedside microdialysis: a tool to monitor cerebral metabolism in subarachnoid hemorrhage patients? *Crit Care Med* 30: 1062–1070, 2002.
31. **Shindo T, Akiyama T, Yamazaki T, and Ninomiya I.** Increase in myocardial norepinephrine during a short period of coronary occlusion. *J Auton Nerv Syst* 48: 91–96, 1994.
32. **Shindo T, Akiyama T, Yamazaki T, and Ninomiya I.** Regional myocardial interstitial norepinephrine kinetics during coronary occlusion and reperfusion. *Am J Physiol Heart Circ Physiol* 270: H245–H251, 1996.
33. **Shirato C, Miura T, Ooiwa H, Toyofuku T, Wilborn WH, and Downey JM.** Tetrazolium artifactually indicates superoxide dismutase-induced salvage in reperfused rabbit heart. *J Mol Cell Cardiol* 21: 1187–1193, 1989.
34. **Spangenthal EJ and Ellis AK.** Cardiac and skeletal muscle myoglobin release after reperfusion of injured myocardium in dogs with systemic hypotension. *Circulation* 91: 2635–2641, 1995.
35. **Steenbergen C, Hill ML, and Jennings RB.** Volume regulation and plasma membrane injury in aerobic, anaerobic, and ischemic myocardium in vitro. Effects of osmotic cell swelling on plasma membrane integrity. *Circ Res* 57: 864–875, 1985.
36. **Takami H, Matsuda H, Kuki S, Nishimura M, Kawashima Y, Watari H, Furuya E, and Tagawa K.** Leakage of cytoplasmic enzymes from rat heart by the stress of cardiac beating after increase in cell membrane fragility by anoxia. *Pflügers Arch* 416: 144–150, 1990.
37. **Van der Laarse A, van der Wall EE, van den Pol RC, Vermeer F, Verheugt FW, Krauss XH, Bar FW, Hermens WT, Willems GW, and Simoons ML.** Rapid enzyme release from acutely infarcted myocardium after early thrombolytic therapy: washout or reperfusion damage? *Am Heart J* 115: 711–716, 1988.
38. **Van Kreel BK, van den Veen FH, Willems GM, and Hermens WT.** Circulatory models in assessment of cardiac enzyme release in dogs. *Am J Physiol Heart Circ Physiol* 264: H747–H757, 1993.
39. **Van Nieuwenhoven FA, Musters RJ, Post JA, Verkleij AJ, Van der Vusse GJ, and Glatz JF.** Release of proteins from isolated neonatal rat cardiomyocytes subjected to simulated ischemia or metabolic inhibition is independent of molecular mass. *J Mol Cell Cardiol* 28: 1429–1434, 1996.
40. **Wiener BJ.** *Statistical Principles in Experimental Design* (2nd ed.). New York: McGraw-Hill, 1971.
41. **Wikström G, Ronquist G, Nilsson S, Maripu E, and Waldenström A.** Continuous monitoring of energy metabolites using microdialysis during myocardial ischaemia in the pig. *Eur Heart J* 16: 339–347, 1995.
42. **Wittenberg JB and Wittenberg BA.** Myoglobin function reassessed. *J Exp Biol* 206: 2011–2020, 2003.
43. **Wu AH.** Biochemical markers of cardiac damage: from traditional enzymes to cardiac-specific proteins. IFCC Subcommittee on Standardization of Cardiac Markers (S-SCM). *Scand J Clin Lab Invest Suppl* 230: 74–82, 1999.
44. **Wunderlich C, Flögel U, Gödecke A, Heger J, and Schrader J.** Acute inhibition of myoglobin impairs contractility and energy state of iNOS-overexpressing hearts. *Circ Res* 92: 1352–1358, 2003.

Am J Physiol Regul Integr Comp Physiol 288: R1432–R1437, 2005;
doi:10.1152/ajpregu.00662.2004.

Adrenomedullin: angiogenesis and gene therapy

Noritoshi Nagaya,[1,2] Hidezo Mori,[3] Shinsuke Murakami,[1] Kenji Kangawa,[4] and Soichiro Kitamura[5]

[1]Department of Regenerative Medicine and Tissue Engineering, [2]Department of Internal Medicine, [3]Department of Cardiac Physiology, [4]Department of Biochemistry, [5]Department of Cardiovascular Surgery, National Cardiovascular Center Research Institute, Osaka, Japan

Nagaya, Noritoshi, Hidezo Mori, Shinsuke Murakami, Kenji Kangawa, and Soichiro Kitamura. Adrenomedullin: angiogenesis and gene therapy. *Am J Physiol Regul Integr Comp Physiol* 288: R1432–R1437, 2005; doi:10.1152/ajpregu.00662.2004.—Adrenomedullin (AM) is a potent, long-lasting vasodilator peptide that was originally isolated from human pheochromocytoma. AM signaling is of particular significance in endothelial cell biology since the peptide protects cells from apoptosis, promotes angiogenesis, and affects vascular tone and permeability. The angiogenic effect of AM is mediated by activation of Akt, mitogen-activated protein kinase/extracellular signal-regulated kinase 1/2, and focal adhesion kinase in endothelial cells. Both AM and its receptor, calcitonin receptor-like receptor, are upregulated through a hypoxia-inducible factor-1-dependent pathway under hypoxic conditions. Thus AM signaling plays an important role in the regulation of angiogenesis in hypoxic conditions. Recently, we have developed a nonviral vector, gelatin. Positively charged gelatin holds negatively charged plasmid DNA in its lattice structure. DNA-gelatin complexes can delay gene degradation, leading to efficient gene transfer. Administration of AM DNA-gelatin complexes induces potent angiogenic effects in a rabbit model of hindlimb ischemia. Thus gelatin-mediated AM gene transfer may be a new therapeutic strategy for the treatment of tissue ischemia. Endothelial progenitor cells (EPCs) play an important role in endothelial regeneration. Interestingly, EPCs phagocytose ionically linked DNA-gelatin complexes in coculture, which allows nonviral gene transfer into EPCs. AM gene transfer into EPCs inhibits cell apoptosis and induces proliferation and migration, suggesting that AM gene transfer strengthens the therapeutic potential of EPCs. Intravenous administration of AM gene-modified EPCs regenerate pulmonary endothelium, resulting in improvement of pulmonary hypertension. These results suggest that in vivo and in vitro transfer of AM gene using gelatin may be applicable for intractable cardiovascular disease.

regeneration; endothelium; ischemia; pulmonary hypertension

ADRENOMEDULLIN (AM) IS A POTENT, long-lasting vasodilator peptide that was originally isolated from human pheochromocytoma (36). The peptide consists of 52 amino acids with an intramolecular disulfide bond, sharing slight homology with calcitonin gene-related peptide and amylin. Immunoreactive AM is detected in plasma and a variety of tissues including, blood vessels, heart, and lungs (19). Particularly, AM shows a variety of effects on the vasculature that include vasodilatation (23), regulation of permeability (16), inhibition of endothelial apoptosis (31), and promotion of angiogenesis (1, 35, 60). In addition, AM has protective effects against vascular injury, including oxidative stress (33, 69, 84). It is becoming clear that either activation or disruption of AM signaling might contribute to many pathological conditions, including hypertension (22), congestive heart failure (55), pulmonary hypertension (29), neoplastic growth (39), and inflammatory disease (59). To date, the major biological acitivities of AM in vitro and in vivo are *1)* vasodilation, *2)* diuresis and natriuresis, *3)* positive inotropic effect, *4)* inhibition of endothelial cell apoptosis, *5)* induction of angiogenesis, *6)* inhibition of cardiomyocyte apoptosis, *7)* suppression of aldosterone production, *8)* anti-inflammatory activity, and *9)* antioxidant activity. We and others have demonstrated that intravenous administration of AM decreases systemic and pulmonary arterial pressure and induces diuresis and natriuresis (47, 52, 65), suggesting that AM is involved in the regulation of vascular tone and body fluid. Subsequent studies have demonstrated beneficial hemodynamic effects and direct cardioprotective effects of AM infusion in the treatment of congestive heart failure (57, 61–64).

Until recently, only vascular endothelial growth factor (VEGF) (80), fibroblast growth factor (68), platelet-derived growth factor (37), and angiopoietin (74) were known to have profound angiogenic effects. More recently, however, the angiogenic potential of AM has attracted investigators' attention (35, 41, 59, 81). A previous study has shown that vascular abnormalities are present in homozygous AM knockout mice (70), suggesting that AM is essential for vascular morphogenesis. AM activates the PI3K/Akt-dependent pathway in vascular endothelial cells (58), which is considered to regulate multiple critical steps in angiogenesis, including endothelial cell survival, proliferation, migration, and capillary-like structure formation (27). These findings raise the possibility that AM plays a role in modulating angiogenesis and neovascular-

Address for reprint requests and other correspondence: Noritoshi Nagaya, Dept. of Regenerative Medicine and Tissue Engineering, National Cardiovascular Center Research Institute, 5-7-1 Fujishirodai, Suita, Osaka 565-8565, Japan (E-mail: nnagaya@ri.ncvc.go.jp).

ization. This review focused on the angiogenic effects of AM and the therapeutic potential of AM gene transfer for the treatment of intractable cardiovascular disease.

ENDOGENOUS AM PRODUCTION IN ISCHEMIC CONDITIONS

Hypoxia (14, 53) and cytokine production (73) in ischemic heart disease or septic shock, as well as shear stress (7) in hypertension and heart failure induce AM secretion by vascular cells (Fig. 1). We have shown that plasma AM level is increased in patients with acute myocardial infarction (40, 49), peripheral arterial occlusive disease (75), and congestive heart failure (28, 55). Tissue levels of AM peptide and mRNA are also markedly increased in ischemic myocardium (18, 50) and failing heart (8, 56, 78, 82). These findings suggest that expression of AM is upregulated under tissue ischemia and inflammation, both of which are associated with neovascularization. An in vitro study has demonstrated that AM is upregulated through a hypoxia-inducible factor-1 (HIF-1)-dependent pathway under hypoxic conditions (14). Thus hypoxia/HIF-1 is one of the most potent regulators of AM production (Fig. 1). A recent study has demonstrated that heterozygous AM knockout mice [AM(+/−)] show significantly less blood flow recovery with less collateral capillary development than their wild-type mice (20). Administration of AM promotes blood flow recovery and capillary formation in AM(+/−) mice. These findings suggest that endogenous AM may play an important role in the regulation of angiogenesis under ischemic conditions. Considering the angiogenic potency of AM, increased endogenous AM represents a compensatory mechanism as an angiogenic factor promoting neovascularization under hypoxic conditions.

ANGIOGENIC EFFECTS OF AM AND ITS SIGNALING PATHWAY

AM signaling is of particular significance in endothelial cell biology since the peptide protects cells from apoptosis (31), promotes angiogenesis (35, 60), and affects vascular tone (23). Angiogenesis is a multistep process that involves migration and proliferation of endothelial cells, functional maturation of the newly assembled vessels, and remodeling of the extracellular matrix (26). Akt, mitogen-activated protein kinase (MAPK)/extracellular signal-regulated kinase 1/2 (ERK1/2), and focal adhesion kinase (p125FAK) play an important role in angiogenesis in endothelial cells. Kim et al. (35) demonstrated that AM activated Akt, MAPK/ERK1/2, and p125FAK in human umbilical vein endothelial cells (HUVECs), and produced increases in their DNA synthesis and migration. AM induced tube formation in HUVECs, and its effect was inhibited by pretreatment with a phosphatidylinositol 3′-kinase (PI3K) inhibitor or mitogen-activated protein kinase/extracellular signal-regulated kinase kinase (MEK)1/2 inhibitor. These findings suggest that AM exerts angiogenic activities through activation of Akt, MAPK, and p125FAK in endothelial cells (Fig. 1). In vivo, overexpression of AM augments collateral flow in ischemic tissues partly through activation of endothelial nitric oxide synthase (eNOS) (1). Earlier studies have shown that the vasodilatory effects of AM are mediated by cAMP/protein kinase in smooth muscle cells (SMCs) (23) and by the eNOS/NO pathway in endothelial cells (17). Thus AM-induced angiogenesis and vasodilation may synergistically improve blood perfusion in ischemic tissues.

Recently, a seven-transmembrane G-protein-coupled receptor, calcitonin receptor-like receptor (CRLR), and receptor activity modifying proteins (RAMPs) have been recognized as integral components of the AM signaling system (38, 43). CRLR has demonstrated the expression of the transcript predominantly in microvascular endothelial cells. This finding supports the view that CRLR is potentially a major mediator of the effects of AM on the vasculature. The effect of AM on CRLR is modified by RAMP2 and RAMP3. The angiogenic effect of AM is mediated by CRLR/RAMP2 and CRLR/RAMP3 receptors (Fig. 1). VEGF and AM act synergistically to induce angiogenic-related effects on endothelial cells in vitro (11). However, blocking antibodies to VEGF cannot significantly inhibit AM-induced capillary tube formation by

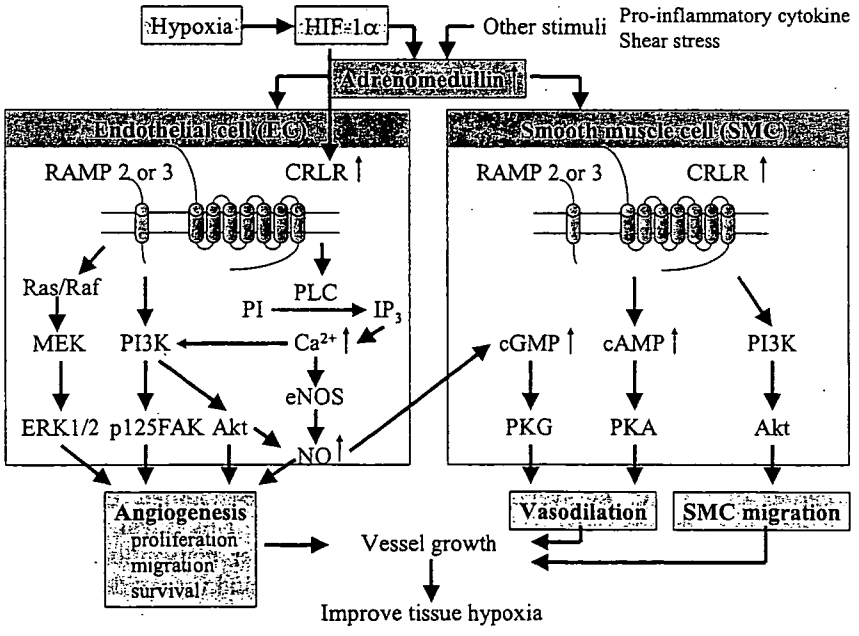

Fig. 1. Signaling pathway of adrenomedullin (AM) in vascular endothelial cells and smooth muscle cells. Both AM and calcitonin-receptor-like receptor (CRLR) are upregulated through a, hypoxia-inducible factor-1 (HIF-1)-dependent pathway under hypoxic conditions. AM binds to CRLR modified by receptor-activity-modifying protein 2 (RAMP2) and RAMP3. AM induces angiogenesis through activation of Akt, MAPK, and p125FAK in endothelial cells. AM also induces SMC migration and vasodilation. These activities synergistically improve tissue ischemia. MEK, mitogen-activated protein kinase/extracellular signal-regulated kinase kinase; ERK, extracellular signal-regulated kinase; PI3K, phosphatidylinositol 3-kinase; p125FAK, focal adhesion kinase; PLC, phospholipase C; PI, phosphatidylinositol; IP_3, inositol triphosphate; eNOS, endothelial nitric oxide synthase; NO, nitric oxide; cGMP, guanosine 3′,5′-cyclic monophosphate; PKG, protein kinase G; PKA, protein kinase A.

HUVECs, indicating that AM does not function indirectly through upregulation of VEGF. Interestingly, AM and CRLR are both upregulated under hypoxic conditions in microvascular endothelial cells, although expression of RAMPs is not activated by hypoxia in microvascular cells (54). The activity of the CRLR promoter under hypoxic conditions is regulated at least in part through hypoxia-responsive regulatory element binding transcription factor HIF-1. Thus the simultaneous transcriptional upregulation of CRLR and its ligand AM in endothelial cells might play a significant role in the vascular responses to hypoxia and ischemia by creating a potent survival loop.

SMCs are essential for the generation of functional and mature blood vessels (26). We demonstrated in vivo that intramuscular administration of AM increased the number of αSMA-positive cells involved in the formation of vascular structures (25). In vitro, AM enhanced SMC migration, which was inhibited by wortmannin, a PI3K inhibitor. Recent studies using homozygous AM knockout mice have suggested that AM is essential for vascular morphogenesis (6, 21, 70). Taking these findings together, it is possible that AM contributes to vessel maturation through enhancement of SMC migration via a PI3K/Akt-dependent pathway (Fig. 1). This feature of AM-induced angiogenesis is different from VEGF-induced angiogenesis, which is not associated with vessel muturation.

In tumor cells, inflammation and hypoxia increase AM expression, and the elevated expression of AM is associated with tumor neovascularization in xenografted endometrial tumors and renal cell carcinoma (12, 86). AM also acts as a tumor cell survival factor underlying human carcinogenesis. Thus hypoxia-induced AM plays a part in tumor angiogenesis in conjunction with VEGF, and facilitates tumor growth under hypoxic conditions. As angiogenesis is an essential process in tumor-host interactions for tumor growth, maintenance, and metastasis, finding ways to regulate the action of AM may provide a new avenue for developing anticancer therapy (16).

THERAPEUTIC ANGIOGENESIS

A variety of studies have demonstrated that AM gene delivery serves as therapeutic tool to protect the cardiovascular system, including the heart (9, 32, 85), kidney (83), and vasculature (2, 84). In this section, we describe the angiogenic potential of AM gene transfer using novel gene delivery systems.

Nonviral gene transfer. Peripheral vascular disease is a crucial health issue affecting an estimated 27 million people (5). Despite recent advances in medical interventions, the symptoms of some patients with critical limb ischemia fail to be controlled. Although gene therapy has been shown to be an effective approach for angiogenesis (10, 24, 72), it is still unsatisfactory because of the biohazard of viral vectors, low transfection efficiency, and premature tissue-targeting. Therefore, highly efficient and safe gene transfer is desirable. Recently, we developed a novel nonviral vector, gelatin hydrogel, which allows highly efficient and long-lasting gene transfer (13, 30, 81). Gelatin has been widely used as a carrier of protein because of its capacity to delay protein degradation (76, 77). Plasmid DNA is known to be negatively charged. Thus we used gelatin as a vector for gene therapy. Biodegradable gelatin was prepared from pig skin. The gelatin was characterized by a spheroid shape with a diameter of ~30 μm, water content of 95% and an isoelectric point of 9 after swelling in water (76, 77). After 2-h incubation, positively charged gelatin held negatively charged plasmid DNA in its positively charged lattice structure. DNA particles are released from the gelatin through its degradation. As a result, DNA-gelatin complexes can delay gene degradation, leading to efficient gene transfer (13, 30, 44, 81).

We examined whether nonviral vector gelatin-mediated AM gene transfer induces therapeutic angiogenesis in a rabbit model of hindlimb ischemia (81). Seven days after intramuscular injection of AM DNA-gelatin complexes, there was intense AM immunoreactivity surrounding the gelatin in the skeletal muscles. AM production in the AM-gelatin group was enhanced compared with that in the naked AM DNA group, which received plasmid AM DNA alone. Unlike AM production in the naked AM group, AM overexpression in the AM-gelatin group lasted for longer than 2 wk. Importantly, AM DNA-gelatin complexes induced more potent angiogenic effects in a rabbit model of hindlimb ischemia than naked AM DNA, as evidenced by significant increases in histological capillary density, calf blood pressure ratio, and laser Doppler flow. These results suggest that the use of biodegradable gelatin as a nonviral vector augments AM expression and enhances AM-induced angiogenic effects. AM DNA-gelatin complexes were distributed mainly in connective tissues. It is interesting to speculate that the delay of gene degradation by gelatin may have been responsible for the highly efficient gene transfer. Thus gelatin-mediated AM gene transfer may be a new therapeutic strategy for the treatment of severe peripheral vascular disease.

Cell-based gene transfer. Recently, transplantation of stem cells or progenitor cells has been shown to regenerate a variety of tissues. Endothelial progenitor cells (EPCs) have been discovered in adult peripheral blood (4, 79). EPCs are mobilized from bone marrow into the peripheral blood in response to tissue ischemia or traumatic injury, migrate to sites of injured endothelium, and differentiate into mature endothelial cells in situ (15, 34). Transplantation of EPC induces therapeutic angiogenesis in the ischemic heart or limb (34, 42, 71). However, some patients are refractory to conventional cell therapy because of insufficient cell number, poor survival, or impaired differentiation. Thus a novel therapeutic strategy to enhance the angiogenic properties of EPCs is desirable. Considering the variety of protective effects of AM on vascular endothelial cells, we hypothesized that AM gene transfer into EPCs would strengthen the therapeutic potential of EPCs. Genetically modified EPCs may serve not only as a tissue-engineering tool to reconstruct the vasculature but also as a vehicle for gene delivery to injured endothelium.

Here, we present a new concept for cell-based gene delivery into the vasculature, consisting of three processes (44). First, positively charged gelatin is readily complexed with negatively charged plasmid DNA. Second, EPCs phagocytose ionically linked plasmid DNA-gelatin complexes in coculture, which allows nonviral gene transfer into EPCs with high efficiency. Third, intravenously administered gene-modified EPCs are incorporated into injured vascular beds. This novel gene delivery system has great advantages over conventional gene therapy; it is nonviral and noninvasive, and it provides highly efficient gene targeting into the vasculature. These benefits

may be achieved mainly by the capability of EPCs to phagocytose DNA-gelatin complexes and to migrate to sites of injured endothelium. Genetically modified EPCs markedly secreted AM into the culture medium, and AM overproduction lasted for more than 2 wk. The proliferative activity of AM DNA-transduced EPCs exceeded that of nontransduced EPCs. Furthermore, AM gene transfer inhibited apoptosis of EPCs in vivo and in vitro. Thus ex vivo AM gene transfer strengthened the therapeutic potential of EPCs.

Primary pulmonary hypertension (PPH) is a rare, but life-threatening disease characterized by progressive pulmonary hypertension, ultimately producing right ventricular failure and death (67). Median survival in patients with PPH is considered to be 2.8 years from the time of diagnosis. Thus novel and effective therapy is needed for the treatment of pulmonary hypertension. Because endothelial dysfunction may play a role in the pathogenesis of pulmonary hypertension such as PPH (3), pulmonary endothelial cells may be a therapeutic target for the treatment of pulmonary hypertension. We have demonstrated that administration of AM peptide decreases pulmonary vascular resistance in patients with PPH (45, 46, 48, 51). Thus we investigated the effects of AM gene-modified EPCs on pulmonary hypertension in rats (44). AM gene-transduced EPCs were similarly incorporated into the pulmonary vasculature. Immunohistochemical analyses demonstrated that the transplanted EPCs were of endothelial lineage and formed vascular structures. Intravenous administration of AM-expressing EPCs significantly decreased pulmonary vascular resistance compared with EPCs alone (−39%). Kaplan-Meier survival curves demonstrated that rats with pulmonary hypertension transplanted with AM-expressing EPCs had a significantly higher survival rate than those given culture medium or EPCs alone. These findings suggest that AM gene-modified EPCs using gelatin may serve not only as a tissue-engineering tool to reconstruct the pulmonary vasculature, but also as a vehicle for gene delivery to injured pulmonary endothelium. This hybrid cell-gene therapy may be applicable for intractable cardiovascular disease, including ischemic heart disease. Thus genetic manipulation of stem cells opens new avenues for regenerative medicine.

GRANTS

This work was supported by the Research Grant for Cardiovascular Disease (16C-6) from the Ministry of Health, Labor and Welfare, Industrial Technology Research Grant Program in 2003 from New Energy and Industrial Technology Development Organization of Japan, Health and Labor Sciences Research Grants-Genome 005, the Mochida Memorial Foundation for Medical and Pharmaceutical Research, and the Promotion of Fundamental Studies in Health Science of the Organization for Pharmaceutical Safety and Research of Japan.

REFERENCES

1. **Abe M, Sata M, Nishimatsu H, Nagata D, Suzuki E, Terauchi Y, Kadowaki T, Minamino N, Kangawa K, Matsuo H, Hirata Y, and Nagai R.** Adrenomedullin augments collateral development in response to acute ischemia. *Biochem Biophys Res Commun* 306: 10–15, 2003.
2. **Agata J, Zhang JJ, Chao J, and Chao L.** Adrenomedullin gene delivery inhibits neointima formation in rat artery after balloon angioplasty. *Regul Pept* 112: 115–120, 2003.
3. **Archer S and Rich S.** Primary pulmonary hypertension: a vascular biology and translational research "work in progress". *Circulation* 102: 2781–2791, 2000.
4. **Asahara T, Murohara T, Sullivan A, Silver M, van der Zee R, Li T, Witzenbichler B, Schatteman G, and Isner JM.** Isolation of putative progenitor endothelial cells for angiogenesis. *Science* 275: 964–967, 1997.
5. **Belch JJ, Topol EJ, Agnelli G, Bertrand M, Califf RM, Clement DL, Creager MA, Easton JD, Gavin 3rd JR, Greenland P, Hankey G, Hanrath P, Hirsch AT, Meyer J, Smith SC, Sullivan F, Weber MA, Prevention of Atherothrombotic, and Disease Network.** Critical issues in peripheral arterial disease detection and management: a call to action. *Arch Intern Med* 163: 884–892, 2003.
6. **Caron KM and Smithies O.** Extreme hydrops fetalis and cardiovascular abnormalities in mice lacking a functional adrenomedullin gene. *Proc Natl Acad Sci USA* 98: 615–619, 2001.
7. **Chun TH, Itoh H, Ogawa Y, Tamura N, Takaya K, Igaki T, Yamashita J, Doi K, Inoue M, Masatsugu K, Korenaga R, Ando J, and Nakao K.** Shear stress augments expression of C-type natriuretic peptide and adrenomedullin. *Hypertension* 29: 1296–1302, 1997.
8. **Cueille C, Pidoux E, de Vernejoul MC, Ventura-Clapier R, and Garel JM.** Increased myocardial expression of RAMP1 and RAMP3 in rats with chronic heart failure. *Biochem Biophys Res Commun* 294: 340–346, 2002.
9. **Dobrzynski E, Wang C, Chao J, and Chao L.** Adrenomedullin gene delivery attenuates hypertension, cardiac remodeling, and renal injury in deoxycorticosterone acetate-salt hypertensive rats. *Hypertension* 36: 995–1001, 2000.
10. **Feldman LJ, Steg PG, Zheng LP, Chen D, Kearney M, McGarr SE, Barry JJ, Dedieu JF, Perricaudet M, and Isner JM.** Low-efficiency of percutaneous adenovirus-mediated arterial gene transfer in the atherosclerotic rabbit. *J Clin Invest* 95: 2662–2671, 1995.
11. **Fernandez-Sauze S, Delfino C, Mabrouk K, Dussert C, Chinot O, Martin PM, Grisoli F, Ouafik L, and Boudouresque F.** Effects of adrenomedullin on endothelial cells in the multistep process of angiogenesis: involvement of CRLR/RAMP2 and CRLR/RAMP3 receptors. *Int J Cancer* 108: 797–804, 2004.
12. **Fujita Y, Mimata H, Nasu N, Nomura T, Nomura Y, and Nakagawa M.** Involvement of adrenomedullin induced by hypoxia in angiogenesis in human renal cell carcinoma. *Int J Urol* 9: 285–295, 2002.
13. **Fukunaka Y, Iwanaga K, Morimoto K, Kakemi M, and Tabata Y.** Controlled release of plasmid DNA from cationized gelatin hydrogels based on hydrogel degradation. *J Control Release* 80: 333–343, 2002.
14. **Garayoa M, Martinez A, Lee S, Pio R, An WG, Neckers L, Trepel J, Montuenga LM, Ryan H, Johnson R, Gassmann M, and Cuttitta F.** Hypoxia-inducible factor-1 (HIF-1) up-regulates adrenomedullin expression in human tumor cell lines during oxygen deprivation: a possible promotion mechanism of carcinogenesis. *Mol Endocrinol* 14: 848–862, 2000.
15. **Gill M, Dias S, Hattori K, Rivera ML, Hicklin D, Witte L, Girardi L, Yurt R, Himel H, and Rafii S.** Vascular trauma induces rapid but transient mobilization of VEGFR2(+)AC133(+) endothelial precursor cells. *Circ Res* 88: 167–174, 2001.
16. **Hippenstiel S, Witzenrath M, Schmeck B, Hocke A, Krisp M, Krull M, Seybold J, Seeger W, Rascher W, Schutte H, and Suttorp N.** Adrenomedullin reduces endothelial hyperpermeability. *Circ Res* 91: 618–625, 2002.
17. **Hirata Y, Hayakawa H, Suzuki Y, Suzuki E, Ikenouchi H, Kohmoto O, Kimura K, Kitamura K, Eto T, Kangawa K, Matsuo H, and Omata M.** Mechanisms of adrenomedullin-induced vasodilation in the rat kidney. *Hypertension* 25: 790–795, 1995.
18. **Hofbauer KH, Jensen BL, Kurtz A, and Sandner P.** Tissue hypoxygenation activates the adrenomedullin system in vivo. *Am J Physiol Regul Integr Comp Physiol* 278: R513–R519, 2000.
19. **Ichiki Y, Kitamura K, Kangawa K, Kawamoto M, Matsuo H, and Eto T.** Distribution and characterization of immunoreactive adrenomedullin in human tissue and plasma. *FEBS Lett* 338: 6–10, 1994.
20. **Iimuro S, Shindo T, Moriyama N, Amaki T, Niu P, Takeda N, Iwata H, Zhang Y, Ebihara A, and Nagai R.** Angiogenic effects of adrenomedullin in ischemia and tumor growth. *Circ Res* 95: 415–423, 2004.
21. **Imai Y, Shiindo T, Maemura K, Kurihara Y, Nagai R, and Kurihara H.** Evidence for the physiological and pathological roles of adrenomedullin from genetic engineering in mice. *Ann NY Acad Sci* 947: 26–33, 2001.
22. **Ishimitsu T, Nishikimi T, Saito Y, Kitamura K, Eto T, Kangawa K, Matsuo H, Omae T, and Matsuoka H.** Plasma levels of adrenomedullin, a newly identified hypotensive peptide, in patients with hypertension and renal failure. *J Clin Invest* 94: 2158–2161, 1994.
23. **Ishizaka Y, Ishizaka Y, Tanaka M, Kitamura K, Kangawa K, Minamino N, Matsuo H, and Eto T.** Adrenomedullin stimulates cyclic AMP formation in rat vascular smooth muscle cells. *Biochem Biophys Res Commun* 200: 642–646, 1994.

24. **Isner JM, Pieczek A, Schainfeld R, Blair R, Haley L, Asahara T, Rosenfield K, Razvi S, Walsh K, and Symes JF.** Clinical evidence of angiogenesis after arterial gene transfer of phVEGF165 in patient with ischemic limb. *Lancet* 348: 370–374, 1996.
25. **Iwase T, Nagaya N, Fujii T, Itoh T, Ishibashi-Ueda H, Yamagishi M, Miyatake K, Matsumoto T, Kitamura S, and Kangawa K.** Adrenomedullin enhances angiogenic potency of bone marrow transplantation in a rat model of hindlimb ischemia. *Circulation* 111: 356–362, 2005.
26. **Jain RK.** Molecular regulation of vessel maturation. *Nat Med* 9: 685–693, 2003.
27. **Jiang BH, Zheng JZ, Aoki M, and Vogt PK.** Phosphatidylinositol 3-kinase signaling mediates angiogenesis and expression of vascular endothelial growth factor in endothelial cells. *Proc Natl Acad Sci USA* 97: 1749–1753, 2000.
28. **Jougasaki M, Wei CM, McKinley LJ, and Burnett JC Jr.** Elevation of circulating and ventricular adrenomedullin in human congestive heart failure. *Circulation* 92: 286–289, 1995.
29. **Kakishita M, Nishikimi T, Okano Y, Satoh T, Kyotani S, Nagaya N, Fukushima K, Nakanishi N, Takishita S, Miyata A, Kangawa K, Matsuo H, and Kunieda T.** Increased plasma levels of adrenomedullin in patients with pulmonary hypertension. *Clin Sci (Lond)* 96: 33–39, 1999.
30. **Kasahara H, Tanaka E, Fukuyama N, Sato E, Sakamoto H, Tabata Y, Ando K, Iseki H, Shinozaki Y, Kimura K, Kuwabara E, Koide S, Nakazawa H, and Mori H.** Biodegradable gelatin hydrogel potentiates the angiogenic effect of fibroblast growth factor 4 plasmid in rabbit hindlimb ischemia. *J Am Coll Cardiol* 41: 1056–1062, 2003.
31. **Kato H, Shichiri M, Marumo F, and Hirata Y.** Adrenomedullin as an autocrine/paracrine apoptosis survival factor for rat endothelial cells. *Endocrinology* 138: 2615–2620, 1997.
32. **Kato K, Yin H, Agata J, Yoshida H, Chao L, and Chao J.** Adrenomedullin gene delivery attenuates myocardial infarction and apoptosis after ischemia and reperfusion. *Am J Physiol Heart Circ Physiol* 285: H1506–H1514, 2003.
33. **Kawai J, Ando K, Tojo A, Shimosawa T, Takahashi K, Onozato ML, Yamasaki M, Ogita T, Nakaoka T, and Fujita T.** Endogenous adrenomedullin protects against vascular response to injury in mice. *Circulation* 109: 1147–1153 2004.
34. **Kawamoto A, Gwon HC, Iwaguro H, Yamaguchi JI, Uchida S, Masuda H, Silver M, Ma H, Kearney M, Isner JM, and Asahara T.** Therapeutic potential of ex vivo expanded endothelial progenitor cells for myocardial ischemia. *Circulation* 103: 634–637, 2001.
35. **Kim W, Moon SO, Sung MJ, Kim SH, Lee S, So JN, and Park SK.** Angiogenic role of adrenomedullin through activation of Akt, mitogen-activated protein kinase, and focal adhesion kinase in endothelial cells. *FASEB J* 13: 1937–1939, 2003.
36. **Kitamura K, Kangawa K, Kawamoto M, Ichiki Y, Nakamura S, Matsuo H, and Eto T.** Adrenomedullin: a novel hypotensive peptide isolated from human pheochromocytoma. *Biochem Biophys Res Commun* 192: 553–560, 1993.
37. **Marx M, Perlmutter RA, and Madri JA.** Modulation of platelet-derived growth factor receptor expression in microvascular endothelial cells during in vitro angiogenesis. *J Clin Invest* 93: 131–139, 1994.
38. **McLatchie LM, Fraser NJ, Main MJ, Wise A, Brown J, Thompson N, Solari R, Lee MG, and Foord SM.** RAMPs regulate the transport and ligand specificity of the calcitonin-receptor-like receptor. *Nature* 393: 333–339, 1998.
39. **Miller MJ, Martinez A, Unsworth EJ, Thiele CJ, Moody TW, Elsasser T, and Cuttitta F.** Adrenomedullin expression in human tumor cell lines. Its potential role as an autocrine growth factor. *J Biol Chem* 271: 23345–23351, 1996.
40. **Miyao Y, Nishikimi T, Goto Y, Miyazaki S, Daikoku S, Morii I, Matsumoto T, Takishita S, Miyata A, Matsuo H, Kangawa K, and Nonogi H.** Increased plasma adrenomedullin levels in patients with acute myocardial infarction in proportion to the clinical severity. *Heart* 79: 39–44, 1998.
41. **Miyashita K, Itoh H, Sawada N, Fukunaga Y, Sone M, Yamahara K, Yurugi-Kobayashi T, Park K, and Nakao K.** Adrenomedullin provokes endothelial Akt activation and promotes vascular regeneration both in vitro and in vivo. *FEBS Lett* 544: 86–92, 2003.
42. **Murohara T, Ikeda H, Duan J, Shintani S, Sasaki K, Eguchi H, Onitsuka I, Matsui K, and Imaizumi T.** Transplanted cord blood-derived endothelial precursor cells augment postnatal neovascularization. *J Clin Invest* 105: 1527–1536, 2000.
43. **Nagae T, Mukoyama M, Sugawara A, Mori K, Yahata K, Kasahara M, Suganami T, Makino H, Fujinaga Y, Yoshioka T, Tanaka I, and Nakao K.** Rat receptor-activity-modifying proteins (RAMPs) for adrenomedullin/CGRP receptor: cloning and upregulation in obstructive nephropathy. *Biochem Biophys Res Commun* 270: 89–93, 2000.
44. **Nagaya N, Kangawa K, Kanda M, Uematsu M, Horio T, Fukuyama N, Hino J, Harada-Shiba M, Okumura H, Tabata Y, Mochizuki N, Chiba Y, Nishioka K, Miyatake K, Asahara T, Hara H, and Mori H.** Hybrid cell-gene therapy for pulmonary hypertension based on phagocytosing action of endothelial progenitor cells. *Circulation* 108: 889–895, 2003.
45. **Nagaya N, Kyotani S, Uematsu M, Ueno K, Oya H, Nakanishi N, Shirai M, Mori H, Miyatake K, and Kangawa K.** Effects of adrenomedullin inhalation on hemodynamics and exercise capacity in patients with idiopathic pulmonary arterial hypertension. *Circulation* 109: 351–356, 2004.
46. **Nagaya N, Miyatake K, Kyotani S, Nishikimi T, Nakanishi N, and Kangawa K.** Pulmonary vasodilator response to adrenomedullin in patients with pulmonary hypertension. *Hypertens Res* 26 Suppl: S141–S146, 2003.
47. **Nagaya N, Nishikimi T, Horio T, Yoshihara F, Kanazawa A, Matsuo H, and Kangawa K.** Cardiovascular and renal effects of adrenomedullin in rats with heart failure. *Am J Physiol Regul Integr Comp Physiol* 276: R213–R218, 1999.
48. **Nagaya N, Nishikimi T, Uematsu M, Satoh T, Oya H, Kyotani S, Sakamaki F, Ueno K, Nakanishi N, Miyatake K, and Kangawa K.** Hemodynamic and hormonal effects of adrenomedullin in patients with pulmonary hypertension. *Heart* 84: 653–658, 2000.
49. **Nagaya N, Nishikimi T, Uematsu M, Yoshitomi Y, Miyao Y, Miyazaki S, Goto Y, Kojima S, Kuramochi M, Matsuo H, Kangawa K, and Nonogi H.** Plasma adrenomedullin as an indicator of prognosis after acute myocardial infarction. *Heart* 81: 483–487, 1999.
50. **Nagaya N, Nishikimi T, Yoshihara F, Horio T, Morimoto A, and Kangawa K.** Cardiac adrenomedullin gene expression and peptide accumulation after acute myocardial infarction in rats. *Am J Physiol Regul Integr Comp Physiol* 278: R1019–R1026, 2000.
51. **Nagaya N, Okumura H, Uematsu M, Shimizu W, Ono F, Shirai M, Mori H, Miyatake K, and Kangawa K.** Repeated inhalation of adrenomedullin ameliorates pulmonary hypertension and survival in monocrotaline rats. *Am J Physiol Heart Circ Physiol* 285: H2125–H2131, 2003.
52. **Nagaya N, Satoh T, Nishikimi T, Uematsu M, Furuichi S, Sakamaki F, Oya H, Kyotani S, Nakanishi N, Goto Y, Masuda Y, Miyatake K, and Kangawa K.** Hemodynamic, renal, and hormonal effects of adrenomedullin infusion in patients with congestive heart failure. *Circulation* 101: 498–503, 2000.
53. **Nakayama M, Takahashi K, Murakami O, Shirato K, and Shibahara S.** Induction of adrenomedullin by hypoxia and cobalt chloride in human colorectal carcinoma cells. *Biochem Biophys Res Commun* 243: 514–517, 1998.
54. **Nikitenko LL, Smith DM, Bicknell R, and Rees MC.** Transcriptional regulation of the CRLR gene in human microvascular endothelial cells by hypoxia. *FASEB J* 17: 1499–501, 2003.
55. **Nishikimi T, Saito Y, Kitamura K, Ishimitsu T, Eto T, Kangawa K, Matsuo H, Omae T, and Matsuoka H.** Increased plasma levels of adrenomedullin in patients with heart failure. *J Am Coll Cardiol* 26: 1424–1431, 1995.
56. **Nishikimi T, Tadokoro K, Mori Y, Wang X, Akimoto K, Yoshihara F, Minamino N, Kangawa K, and Matsuoka H.** Ventricular adrenomedullin system in the transition from LVH to heart failure in rats. *Hypertension* 41: 512–518, 2003.
57. **Nishikimi T, Yoshihara F, Horinaka S, Kobayashi N, Mori Y, Tadokoro K, Akimoto K, Minamino N, Kangawa K, and Matsuoka H.** Chronic administration of adrenomedullin attenuates transition from left ventricular hypertrophy to heart failure in rats. *Hypertension* 42: 1034–1041, 2003.
58. **Nishimatsu H, Suzuki E, Nagata D, Moriyama N, Satonaka H, Walsh K, Sata M, Kangawa K, Matsuo H, Goto A, Kitamura T, and Hirata Y.** Adrenomedullin induces endothelium-dependent vasorelaxation via the phosphatidylinositol 3-kinase/Akt-dependent pathway in rat aorta. *Circ Res* 89: 63–70, 2001.
59. **Nishio K, Akai Y, Murao Y, Doi N, Ueda S, Tabuse H, Miyamoto S, Dohi K, Minamino N, Shoji H, Kitamura K, Kangawa K, and Matsuo H.** Increased plasma concentrations of adrenomedullin correlate with relaxation of vascular tone in patients with septic shock. *Crit Care Med* 25: 953–957, 1997.

60. **Oehler MK, Hague S, Rees MC, and Bicknell R.** Adrenomedullin promotes formation of xenografted endometrial tumors by stimulation of autocrine growth and angiogenesis. *Oncogene* 21: 2815–2821, 2002.
61. **Okumura H, Nagaya N, Itoh T, Okano I, Hino J, Mori K, Tsukamoto Y, Ishibashi-Ueda H, Miwa S, Tambara K, Toyokuni S, Yutani C, and Kangawa K.** Adrenomedullin infusion attenuates myocardial ischemia/reperfusion injury through the phosphatidylinositol 3-kinase/Akt-dependent pathway. *Circulation* 109: 242–248, 2004.
62. **Rademaker MT, Cameron VA, Charles CJ, Lainchbury JG, Nicholls MG, and Richards AM.** Adrenomedullin and heart failure. *Regul Pept* 112: 51–60, 2003.
63. **Rademaker MT, Charles CJ, Cooper GJ, Coy DH, Espiner EA, Lewis LK, Nicholls MG, and Richards AM.** Combined angiotensin-converting enzyme inhibition and adrenomedullin in an ovine model of heart failure. *Clin Sci (Lond)* 102: 653–660, 2002.
64. **Rademaker MT, Charles CJ, Espiner EA, Nicholls MG, and Richards AM.** Long-term adrenomedullin administration in experimental heart failure. *Hypertension* 40: 667–672, 2002.
65. **Rademaker MT, Charles CJ, Lewis LK, Yandle TG, Cooper GJ, Coy DH, Richards AM, and Nicholls MG.** Beneficial hemodynamic and renal effects of adrenomedullin in an ovine model of heart failure. *Circulation* 96: 1983–1990, 1997.
66. **Ribatti D, Guidolin D, Conconi MT, Nico B, Baiguera S, Parnigotto PP, Vacca A, and Nussdorfer GG.** Vinblastine inhibits the angiogenic response induced by adrenomedullin in vitro and in vivo. *Oncogene* 22: 6458–6461, 2003.
67. **Rich S, Dantzker DR, Ayres SM, Bergofsky EH, Brundage BH, Detre KM, Fishman AP, Goldring RM, Groves BM, Koerner SK, Levy PC, Reid LM, Vreim CE, and Williams GW.** Primary pulmonary hypertension : a national prospective study. *Ann Intern Med* 107: 216–223, 1987.
68. **Schweigerer L, Neufeld G, Friedman J, Abraham JA, Fiddes JC, and Gospodarowicz D.** Capillary endothelial cells express basic fibroblast growth factor, a mitogen that promotes their own growth. *Nature* 325: 257–259, 1987.
69. **Shimosawa T, Shibagaki Y, Ishibashi K, Kitamura K, Kangawa K, Kato S, Ando K, and Fujita T.** Adrenomedullin, an endogenous peptide, counteracts cardiovascular damage. *Circulation* 105:106–111, 2002.
70. **Shindo T, Kurihara Y, Nishimatsu H, Moriyama N, Kakoki M, Wang Y, Imai Y, Ebihara A, Kuwaki T, Ju KH, Minamino N, Kangawa K, Ishikawa T, Fukuda M, Akimoto Y, Kawakami H, Imai T, Morita H, Yazaki Y, Nagai R, Hirata Y, and Kurihara H.** Vascular abnormalities and elevated blood pressure in mice lacking adrenomedullin gene. *Circulation* 104: 1964–1971, 2001.
71. **Shintani S, Murohara T, Ikeda H, Ueno T, Sasaki K, Duan J, and Imaizumi T.** Augmentation of postnatal neovascularization with autologous bone marrow transplantation. *Circulation* 103: 897–903, 2001.
72. **St George JA.** Gene therapy progress and prospects: adenoviral vectors. *Gene Ther* 10: 1135–1141, 2003.
73. **Sugo S, Minamino N, Shoji H, Kangawa K, Kitamura K, Eto T, and Matsuo H.** Interleukin-1, tumor necrosis factor and lipopolysaccharide additively stimulate production of adrenomedullin in vascular smooth muscle cells. *Biochem Biophys Res Commun* 207: 25–32, 1995.
74. **Suri C, Jones PF, Patan S, Bartunkova S, Maisonpierre PC, Davis S, Sato TN, and Yancopoulos GD.** Requisite role of angiopoietin-1, a ligand for the TIE2 receptor, during embryonic angiogenesis. *Cell* 87: 1171–1180, 1996.
75. **Suzuki Y, Horio T, Hayashi T, Nonogi H, Kitamura K, Eto T, Kangawa K, and Kawano Y.** Plasma adrenomedullin concentration is increased in patients with peripheral arterial occlusive disease associated with vascular inflammation. *Regul Pept* 118: 99–104, 2004.
76. **Tabata Y and Ikada Y.** Macrophage activation through phagocytosis of muramyl dipeptide encapsulated in gelatin microspheres. *J Pharm Pharmacol* 39: 698–704, 1987.
77. **Tabata Y, Nagano A, and Ikada Y.** Biodegradation of hydrogel carrier incorporating fibroblast growth factor. *Tissue Eng* 5: 127–138, 1999.
78. **Tadokoro K, Nishikimi T, Mori Y, Wang X, Akimoto K, and Matsuoka H.** Altered gene expression of adrenomedullin and its receptor system and molecular forms of tissue adrenomedullin in left ventricular hypertrophy induced by malignant hypertension. *Regul Pept* 112: 71–78, 2003.
79. **Takahashi T, Kalka C, Masuda H, Chen D, Silver M, Kearney M, Magner M, Isner JM, and Asahara T.** Ischemia- and cytokine-induced mobilization of bone marrow-derived endothelial progenitor cells for neovascularization. *Nat Med* 5: 434–438, 1999.
80. **Takeshita S, Zheng LP, Brogi E, Kearney M, Pu LQ, Bunting S, Ferrara N, Symes JF, and Isner JM.** Therapeutic angiogenesis. A single intra-arterial bolus of vascular endothelial growth factor augments revascularization in a rabbit ischemic hind limb model. *J Clin Invest* 93: 662–670, 1994.
81. **Tokunaga N, Nagaya N, Shirai M, Tanaka E, Ishibashi-Ueda H, Harada-Shiba M, Kanda M, Ito T, Shimizu W, Tabata Y, Uematsu M, Nishigami K, Sano S, Kangawa K, and Mori H.** Adrenomedullin gene transfer induces therapeutic angiogenesis in a rabbit model of chronic hind limb ischemia: benefits of a novel nonviral vector, gelatin. *Circulation* 109: 526–531, 2004.
82. **Totsune K, Takahashi K, Mackenzie HS, Murakami O, Arihara Z, Sone M, Mouri T, Brenner BM, and Ito S.** Increased gene expression of adrenomedullin and adrenomedullin-receptor complexes, receptor-activity modifying protein (RAMP)2 and calcitonin-receptor-like receptor (CRLR) in the hearts of rats with congestive heart failure. *Clin Sci (Lond)* 99: 541–546, 2000.
83. **Wang C, Dobrzynski E, Chao J, and Chao L.** Adrenomedullin gene delivery attenuates renal damage and cardiac hypertrophy in Goldblatt hypertensive rats. *Am J Physiol Renal Physiol* 280: F964–F971, 2001.
84. **Yamasaki M, Kawai J, Nakaoka T, Ogita T, Tojo A, and Fujita T.** Adrenomedullin overexpression to inhibit cuff-induced arterial intimal formation. *Hypertension* 41: 302–307, 2003.
85. **Yin H, Chao L, and Chao J.** Adrenomedullin protects against myocardial apoptosis after ischemia/reperfusion through activation of Akt-GSK signaling. *Hypertension* 43: 109–116, 2004.
86. **Zudaire E, Martinez A, and Cuttitta F.** Adrenomedullin and cancer. *Regul Pept* 112: 175–183, 2003.

Annual Report of Iwate Medical University
School of Liberal Arts and Sciences
No. 40(2005), 1 - 7.

X-ray Spectra from a Characteristic X-ray Generator with a Molybdenum Tube

Eiichi Sato[a], Etsuro Tanaka[b], Hidezo Mori[c], Toshiaki Kawai[d], Takashi Inoue[e], Akira Ogawa[e], Kiyomi Takahashi[f], Shigehiro Sato[f] and Kazuyoshi Takayama[g]

(Received October 31, 2005)

Abstract

This generator consists of the following components: a constant high-voltage power supply, a filament power supply, a turbomolecular pump, and an x-ray tube. The x-ray tube is a demountable diode which is connected to the turbomolecular pump and consists of the following major devices: a molybdenum rod target, a tungsten hairpin cathode (filament), a focusing electrode, a polyethylene terephthalate x-ray window 0.25 mm in thickness, and a stainless-steel tube body. In the x-ray tube, the positive high voltage is applied to the anode (target) electrode, and the cathode is connected to the tube body (ground potential). In this experiment, the tube voltage applied was from 22 to 36 kV, and the tube current was regulated to within 100 μA by the filament temperature. The exposure time is controlled in order to obtain optimum x-ray intensity. The electron beams from the cathode are converged to the target by the focusing electrode, and x-rays are produced through the focusing electrode. Using a lithium fluoride curved crystal, clean K-series characteristic x-rays were observed without using a filter. However, bremsstrahlung x-rays were observed using a cadmium telluride detector.

Keywords: demountable x-ray tube, quasi-monochromatic x-rays, K-series characteristic x-rays, Sommerfeld's theory, curved crystal, cadmium telluride detector

1. Introduction

Most flash x-ray generators employ high-voltage condensers and cold-cathode x-ray tubes,[1-5] and the plasma x-ray source has been growing with increases in the electrostatic energy in the condenser. By

[a] Department of Physics, Iwate Medical University, 3-16-1 Honchodori, Morioka 020-0015, Japan
[b] Department of Nutritional Science, Faculty of Applied Bio-science, Tokyo University of Agriculture, 1-1-1 Sakuragaoka, Setagaya-ku 156-8502, Japan
[c] Department of Cardiac Physiology, National Cardiovascular Center Research Institute, 5-7-1 Fujishirodai, Suita, Osaka 565-8565, Japan
[d] Electron Tube Division #2, Hamamatsu Photonics K. K., 314-5 Shimokanzo, Iwata 438-0193, Japan
[e] Department of Neurosurgery, School of Medicine, Iwate Medical University, 19-1 Uchimaru, Morioka 020-8505, Japan
[f] Department of Microbiology, School of Medicine, Iwate Medical University, 19-1 Uchimaru, Morioka 020-8505, Japan
[g] Shock Wave Research Center, Institute of Fluid Science, Tohoku University, 2-1-1 Katahira, Sendai 980-8577, Japan

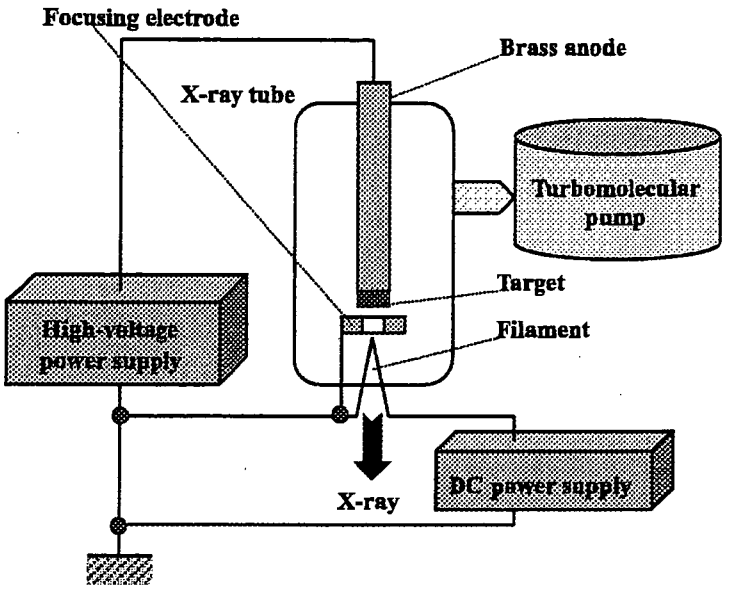

Fig. 1: Block diagram including the main transmission line of the compact x-ray generator with a quasi-monochromatic diode.

forming weakly ionized linear plasma[6-9] using a rod-target triode, we confirmed irradiation of clean K-series characteristic x-rays such as hard x-ray lasers and their higher harmonic hard x-rays from the plasma axial direction. Because the plasma transmits high-photon-energy bremsstrahlung x-rays, it is difficult to produce high-photon-energy characteristic x-rays. In view of this situation, we have developed a super-fluorescent x-ray generator[10-13] by forming weakly ionized plasma at the target tip and have succeeded in producing comparatively clean K-series characteristic x-rays of molybdenum, cerium, tantalum, and tungsten. In particular, the cerium target is useful for performing iodine K-edge angiography, and gadolinium K-edge angiography can be performed using tantalum and tungsten targets.

Steady-state K-series characteristic x-rays left by filters have been employed to perform mammography using a molybdenum target and to perform K-edge angiography[14-17] using a cerium target. In addition, the rays are also useful for performing real-time radiography achieved with a flat panel detector. Because the characteristic x-ray intensity decreases with increases in the filter thickness, the development of a characteristic x-ray generator utilizing the angle dependence of bremsstrahlung x-rays has been wished for.

In the spectrum measurements, we employ a cadmium telluride detector and a lithium fluoride curved crystal. The detector is useful to measure the total spectra including scattering beams. On the other hand, the spectra from only the x-ray source can be measured using the crystal by selecting Bragg's angle.

In this paper, we describe an x-ray generator developed and used to perform a preliminary experiment for generating clean K-series characteristic x-rays by angle dependence of the bremsstrahlung x-rays and measurement of the x-ray spectra using two methods.

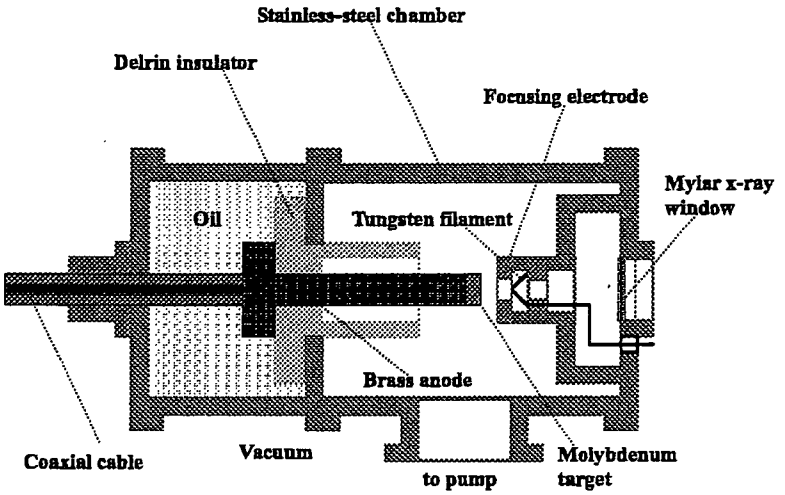

Fig. 2: Schematic drawing of the quasi-monochromatic x-ray tube.

2. Generator

Figure 1 shows a block diagram of a compact characteristic (quasi-monochromatic) x-ray generator. This generator consists of the following components: a constant high-voltage power supply (SL150, Spellman Inc.), a DC filament power supply, a turbomolecular pump, and an x-ray tube. The structure of the x-ray tube is illustrated in Fig. 2. The x-ray tube is a demountable diode which is connected to the turbomolecular pump with a pressure of approximately 0.5 mPa and consists of the following major devices: a molybdenum plate target, a tungsten hairpin cathode (filament), a focusing electrode, a polyethylene terephthalate x-ray window 0.25 mm in thickness, and a stainless-steel tube body. In the x-ray tube, the positive high voltage is applied to the anode (target) electrode, and the cathode is connected to the tube body (ground potential). In this experiment, the tube voltage applied was from 22 to 36 kV, and the tube current was regulated to within 100 μA by the filament temperature. The exposure time is controlled in order to obtain optimum x-ray intensity. The electron beams from the cathode are converged to the target by the focusing electrode, and x-rays are produced through the focusing electrode. Because bremsstrahlung rays are not emitted in the opposite direction to that of electron trajectory, clean molybdenum K-series x-rays can be produced without using a filter.

3. Characteristics

3.1 X-ray intensity

X-ray intensity was measured by a Victoreen 660 ionization chamber at 1.0 m from the x-ray source (Fig. 3). At a constant tube current of 100 μA, the x-ray intensity increased when the tube voltage was

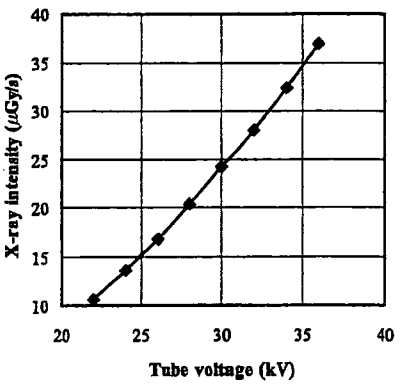

Fig. 3: X-ray intensity at 1.0 m from the x-ray source according to changes in the tube voltage.

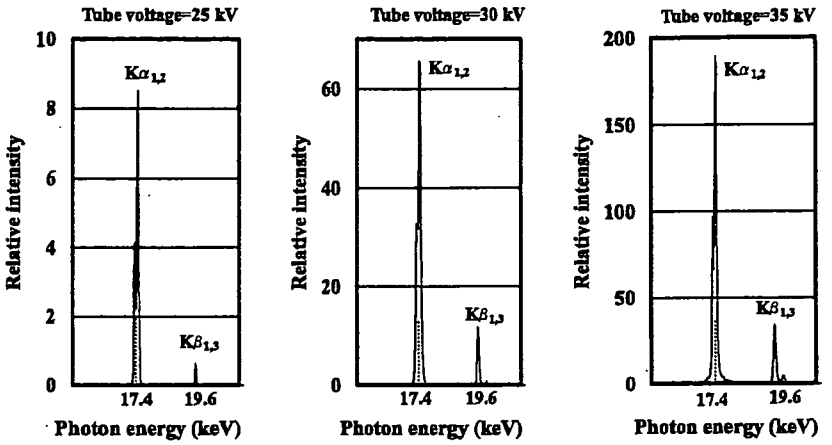

Fig. 4: X-ray spectra from the molybdenum target measured using a transmission type spectrometer with a lithium fluoride curved crystal.

increased. In this measurement, the intensity with a tube voltage of 30 kV and a current of 100 μA was 24.2 μGy/s at 1.0 m from the source.

3.2 X-ray spectra

First, x-ray spectra were measured using a transmission-type spectrometer with a lithium fluoride curved crystal 0.5 mm in thickness. The x-ray intensities of the spectra were detected by an imaging plate of the CR system[18] (Konica Minolta Regius 150) with a wide dynamic range, and relative x-ray intensity was calculated from Dicom original digital data corresponding to x-ray intensity. Figure 4 shows measured spectra from the molybdenum target. We observed clean K lines, while bremsstrahlung

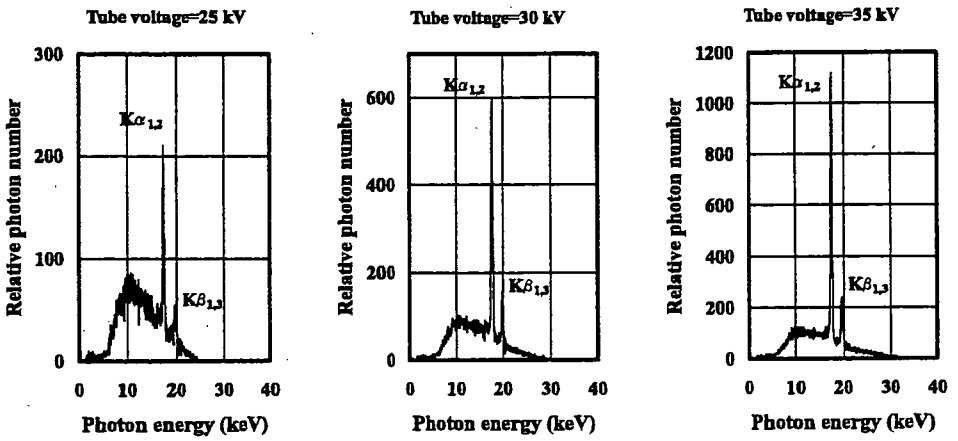

Fig. 5: X-ray spectra from the molybdenum target measured using a cadmium telluride detector.

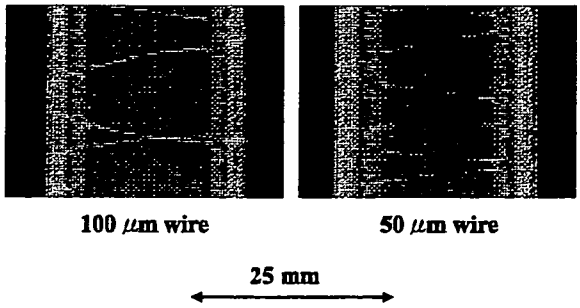

Fig. 6: Radiograms of tungsten wires of 50 and 100 μm in diameter coiled around pipes made of polymethyl methacrylate. A 50-μm-diameter wire could be observed.

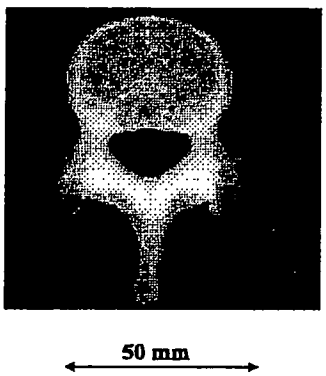

Fig. 7: Radiogram of a vertebra. Fine structure of the vertebra were visible.

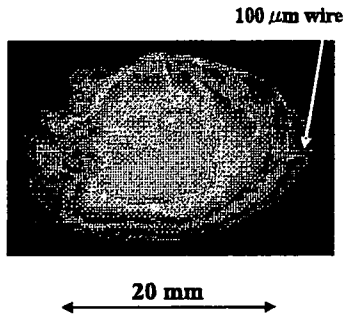

Fig. 8: Angiograms of a rabbit heart. Coronary arteries were visible.

rays were hardly detected. The characteristic x-ray intensity substantially increased with increases in the tube voltage.

The measured spectra using a cadmium telluride detector are shown in Fig. 5. Using the detector, we observed low intensity continuous x-rays. When the tube voltage was increased, both the characteristic x-ray intensity and the maximum photon energy increased.

4. Radiography

The monochromatic radiography was performed by the CR system at 1.0 m from the x-ray source with the filter, and the tube voltage was 30 kV.

First, rough measurements of image resolution were made using wires. Figure 6 shows radiograms of tungsten wires coiled around pipes made of polymethyl methacrylate (PMMA). Although the image contrast increased with increases in the wire diameter, a 50-μm-diameter wire could be observed.

A radiogram of a vertebra is shown in Fig. 7, and the fine structure of the vertebra was observed. Next, angiography was performed using iodine microspheres of 15 μm in diameter. Figure 8 shows an angiogram of a rabbit heart, and we obtained high contrast images of coronary arteries and fine blood vessels.

5. Conclusions and Outlook

In summary, we developed a new characteristic x-ray generator with a molybdenum-target tube and measured clean molybdenum K lines using the crystal spectrometer. However, continuous x-rays were detected using the detector. In both measurements, the characteristic x-ray intensity increased with increases in the tube voltage, and monochromatic $K\alpha$ lines were left by a zirconium filter. Because we could measure bremsstrahlung x-rays[19] from a transmission-type molybdenum target using the crystal, the bremsstrahlung intensity was low as compared with that obtained using conventional molybdenum tubes.

In this preliminary experiment, although the maximum tube voltage and current were 36 kV and 100 μA, the voltage and current could be increased to 100 kV and 1.0 mA, respectively. Under the pulsed operation, the current can be increased to approximately 1 A without considering the target evaporation. Subsequently, the generator produced maximum number of characteristic photons was approximately 1×10^6 photons/($cm^2 \cdot s$) at 1.0 m from the source, and the photon count rate can be increased easily by increasing the current.

Using this x-ray generator, because it is not easy to produce high-photon-energy K-series characteristic x-rays, we are very interested in increasing the energy by changing the electrode configuration between the target, cathode, and focusing electrodes.

Acknowledgments

This work was supported by Grants-in-Aid for Scientific Research (13470154, 13877114, 16591181, and 16591222) and Advanced Medical Scientific Research from MECSST, Health and Labor Sciences Research Grants (RAMT-nano-001, RHGTEFB-genome-005 and RHGTEFB-saisei-003), Grants from the Keiryo Research Foundation, The Promotion and Mutual Aid Corporation for Private Schools of Japan, Japan Science and Technology Agency (JST), and The New Energy and Industrial Technology Development Organization (NEDO, Industrial Technology Research Grant Program in '03).

References

1. R. Germer, "X-ray flash techniques," *J. Phys. E: Sci. Instrum.*, **12**, 336-350, 1979.
2. E. Sato, S. Kimura, S. Kawasaki, H. Isobe, K. Takahashi, Y. Tamakawa and T. Yanagisawa, "Repetitive flash x-ray generator utilizing a simple diode with a new type of energy-selective function," *Rev. Sci. Instrum.*, **61**, 2343-2348, 1990.
3. A. Shikoda, E. Sato, M. Sagae, T. Oizumi, Y. Tamakawa and T. Yanagisawa, "Repetitive flash x-ray generator having a high-durability diode driven by a two-cable-type line pulser," *Rev. Sci. Instrum.*, **65**, 850-856, 1994.
4. E. Sato, K. Takahashi, M. Sagae, S. Kimura, T. Oizumi, Y. Hayasi, Y. Tamakawa and T. Yanagisawa, "Sub-kilohertz flash x-ray generator utilizing a glass-enclosed cold-cathode triode," *Med. & Biol. Eng. & Comput.*, **32**, 289-294, 1994.
5. K. Takahashi, E. Sato, M. Sagae, T. Oizumi, Y. Tamakawa and T. Yanagisawa, "Fundamental study on a long-duration flash x-ray generator with a surface-discharge triode," *Jpn. J. Appl. Phys.*, **33**, pp. 4146-4151, 1994.
6. E. Sato, Y. Hayasi, R. Germer, E. Tanaka, H. Mori, T. Kawai, T. Ichimaru, K. Takayama and H. Ido,

"Quasi-monochromatic flash x-ray generator utilizing weakly ionized linear copper plasma," *Rev. Sci. Instrum.*, **74**, 5236-5240, 2003.

7. E. Sato, Y. Hayasi, R. Germer, E. Tanaka, H. Mori, T. Kawai, H. Obara, T. Ichimaru, K. Takayama and H. Ido, "Irradiation of intense characteristic x-rays from weakly ionized linear molybdenum plasma," *Jpn. J. Med. Phys.*, **23**, 123-131, 2003.
8. E. Sato, Y. Hayasi, R. Germer, E. Tanaka, H. Mori, T. Kawai, T. Ichimaru, S. Sato, K. Takayama and H. Ido, "Sharp characteristic x-ray irradiation from weakly ionized linear plasma," *J. Electron Spectrosc. Related Phenom.*, **137-140**, 713-720, 2004.
9. E. Sato, E. Tanaka, H. Mori, T. Kawai, S. Sato and K. Takayama, "Clean monochromatic x-ray irradiation from weakly ionized linear copper plasma," *Opt. Eng.*, **44**, 049002-1-6, 2005.
10. E. Sato, M. Sagae, E. Tanaka, Y. Hayasi, R. Germer, H. Mori, T. Kawai, T. Ichimaru, S. Sato, K. Takayama and H. Ido, "Quasi-monochromatic flash x-ray generator utilizing a disk-cathode molybdenum tube," *Jpn. J. Appl. Phys.*, **43**, 7324-7328, 2004.
11. E. Sato, E. Tanaka, H. Mori, T. Kawai, T. Ichimaru, S. Sato, K. Takayama and H. Ido, "Compact monochromatic flash x-ray generator utilizing a disk-cathode molybdenum tube," *Med. Phys.*, **32**, 49-54, 2005.
12. E. Sato, E. Tanaka, H. Mori, T. Kawai, T. Inoue, A. Ogawa, S. Sato, K. Takayama and H. Ido, "High-speed K-edge angiography achieved with tantalum K-series characteristic x rays," *SPIE*, **5745**, 810-817, 2005.
13. E. Sato, Y. Hayasi, R. Germer, K. Kimura, E. Tanaka, H. Mori, T. Kawai, T. Inoue, A. Ogawa, S. Sato, K. Takayama and H. Ido, "Enhanced K-edge plasma angiography achieved with tungsten Kα rays utilizing gadolinium-based contrast media," *SPIE*, **5920**, 592012-1-8, 2005.
14. E. Sato, Y. Hayasi, R. Germer, E. Tanaka, H. Mori, T. Kawai, T. Ichimaru, S. Sato, K. Takayama and H. Ido, "Portable x-ray generator utilizing a cerium-target radiation tube for angiography," *J. Electron Spectrosc. Related Phenom.*, **137-140**, 699-704, 2004.
15. E. Sato, E. Tanaka, H. Mori, T. Kawai, T. Ichimaru, S. Sato, K. Takayama and H. Ido, "Demonstration of enhanced K-edge angiography using a cerium target x-ray generator," *Med. Phys*, **31**, 3017-3021, 2004.
16. E. Sato, R. Germer, E. Tanaka, H. Mori, T. Kawai, T. Ichimaru, S. Sato, H. Ojima, K. Takayama and H. Ido, "Quasi-monochromatic cerium flash angiography," *SPIE*, **5580**, 146-152, 2005.
17. E. Sato, E. Tanaka, H. Mori, T. Kawai, T. Inoue, A. Ogawa, A. Yamadera, S. Sato. F. Ito, K. Takayama and H. Ido, "Variations in cerium x-ray spectra and enhanced K-edge angiography," *Jpn. J. Appl. Phys*, **44**, 8204-8209, 2005.
18. E. Sato, K. Satoi and Y. Tamakawa, "Film-less computed radiography system for high-speed imaging," *Ann. Rep. Iwate Med. Univ. Sch. Lib. Arts and Sci.*, **35**, 13-23, 2000.
19. M. Sagae, E. Sato, E. Tanaka, Y. Hayasi, R. Germer, H. Mori, T. Kawai, T. Ichimaru, S. Sato, K. Takayama and H. Ido, "Quasi-monochromatic x-ray generator utilizing graphite cathode diode with transmission-type molybdenum target," *Jpn. J. Appl. Phys.*, **44**, 446-449, 2005.

Annual Report of Iwate Medical University
School of Liberal Arts and Sciences
No. 40(2005), 9-15.

Measurement of Cerium X-ray Spectra Using a Cerium Oxide Powder Filter and Enhanced K-edge Angiography

Eiichi Sato[a], Etsuro Tanaka[b], Hidezo Mori[c], Toshiaki Kawai[d], Takashi Inoue[e], Akira Ogawa[e], Kiyomi Takahashi[f], Shigehiro Sato[f] and Kazuyoshi Takayama[g]

(Received October 31, 2005)

Abstract

The cerium-target x-ray tube is useful in order to perform cone-beam K-edge angiography because K-series characteristic x-rays from the cerium target are absorbed effectively by iodine-based contrast media. The x-ray generator consists of a main controller and a unit with a high-voltage circuit and a fixed anode x-ray tube. The tube is a glass-enclosed diode with a cerium target and a 0.5-mm-thick beryllium window. The maximum tube voltage and current were 70 kV and 0.40 mA, respectively, and the focal-spot sizes were approximately 1×1 mm. Cerium K-series characteristic x-rays were left using a cerium oxide powder filter, and the x-ray intensity was 14.3 μGy/s at 1.0 m from the source with a tube voltage of 60 kV, a current of 0.40 mA, and an exposure time of 1.0 s. Angiography was performed with a computed radiography system using iodine-based microspheres 15 μm in diameter. In angiography of non-living animals, we observed fine blood vessels of approximately 100 μm with high contrasts.

Keywords: x-ray tube, cerium target, cerium oxide filter, powder filter, characteristic x-rays, K-edge angiography

1. Introduction

Flash x-ray generators are useful for performing high-speed radiography,[1] and several different generators with maximum photon energies of 150 keV[2-5] have been applied to biomedical radiography. By forming weakly ionized linear plasma[6-9] using a cold-cathode triode, we have succeeded in producing K-series characteristic x-rays of nickel and copper. Subsequently, we have developed super-fluorescent

[a] Department of Physics, Iwate Medical University, 3-16-1 Honchodori, Morioka 020-0015, Japan
[b] Department of Nutritional Science, Faculty of Applied Bio-science, Tokyo University of Agriculture, 1-1-1 Sakuragaoka, Setagaya-ku 156-8502, Japan
[c] Department of Cardiac Physiology, National Cardiovascular Center Research Institute, 5-7-1 Fujishirodai, Suita, Osaka 565-8565, Japan
[d] Electron Tube Division #2, Hamamatsu Photonics K. K., 314-5 Shimokanzo, Iwata 438-0193, Japan
[e] Department of Neurosurgery, School of Medicine, Iwate Medical University, 19-1 Uchimaru, Morioka 020-8505, Japan
[f] Department of Microbiology, School of Medicine, Iwate Medical University, 19-1 Uchimaru, Morioka 020-8505, Japan
[g] Shock Wave Research Center, Institute of Fluid Science, Tohoku University, 2-1-1 Katahira, Sendai 980-8577, Japan

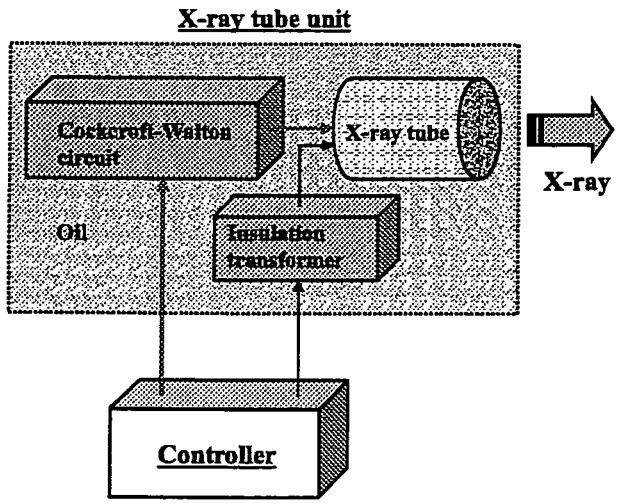

Fig. 1: Block diagram of the compact x-ray generator with a cerium-target radiation tube, which is used specially for K-edge angiography using iodine-based contrast media.

x-ray generator[10-13] to produce comparatively clean high-photon-energy characteristic x-rays of cerium and tungsten.

To produce steady state x-rays, synchrotrons generate high-dose-rate bremsstrahlung x-rays, and monochromatic parallel beams are formed using single crystals. In particular, x-rays of approximately 35 keV have been applied to perform enhanced K-edge angiography[14,15] and phase-contrast radiography,[16,17] including dark-field imaging using an analyzer crystal. Using these imaging, although the spatial resolution has been improved, it is difficult to increase the irradiation field due to the parallelity. Recently, we have developed a steady-state x-ray generator utilizing a cerium-target tube[18-20] and have demonstrated enhanced K-edge angiography utilizing a barium sulfate filter. In this research, $K\alpha$ lines (34.6 keV) were left by absorbing $K\beta$ lines (39.2 keV), and bremsstrahlung x-rays with photon energies lower than the barium K-edge (37.4 keV) were also observed. However, because cerium $K\beta$ lines are also absorbed effectively by iodine, both $K\alpha$ and $K\beta$ lines should be selected to perform angiography. In the present research, we measured the x-ray spectra from a cerium-target tube using a new cadmium telluride detector, and performed a preliminary study on cone-beam K-edge angiography achieved with cerium characteristic x-rays using a cerium oxide powder filter.

2. Generator

Figure 1 shows the block diagram of the x-ray generator, which consists of a main controller and an x-ray tube unit with a Cockcroft-Walton circuit and a cerium-target tube. The tube voltage, the current, and the exposure time can be controlled by the controller. The main circuit for producing x-rays is illustrated in Fig. 2, and employed the Cockcroft-Walton circuit in order to decrease the dimensions of the tube unit. In the x-ray tube, the negative high-voltage is applied to the cathode electrode, and the anode (target) is connected to the tube unit case (ground potential) to cool the anode and the target effectively. The filament heating current is supplied by an AC power supply in the controller in